Rationally Designed Nucleobase and Nucleotide Coordinated Nanoparticles for Selective DNA Adsorption and Detection

Feng Wang, Biwu Liu, Po-Jung Jimmy Huang and Juewen Liu*

Department of Chemistry, Waterloo Institute for Nanotechnology, University of Waterloo, Waterloo, Ontario, Canada, N2L 3G1

Email: liujw@uwaterloo.ca

Abstract.

Nanomaterials for DNA adsorption are useful for sequence-specific DNA detection. Current materials for DNA adsorption employ electrostatic attraction, hydrophobic interaction, or π-π stacking, none of which can achieve sequence specificity. Specificity might be improved by involving hydrogen bonding and metal coordination. In this work, a diverse range of nucleobase/nucleotide (adenine, adenosine, ATP, AMP, and GTP) coordinated materials containing various metal ions (Au(III), Ag(I), Ce(III), Gd(III), and Tb(III)) are prepared. In most cases, nanoparticles are formed. These materials have different surface charges and positively charged particles only show non-specific DNA adsorption. Negatively charged materials give different adsorption kinetics for different DNA sequences, where complementary DNA homopolymers are adsorbed faster than other sequences. Therefore, the bases in the coordinated materials can still form base pairs with the DNA. The adsorption strength is mainly controlled by the metal ions, where Au shows the strongest adsorption while lanthanides are weaker. These materials can

be used as sensors for DNA detection and can also deliver DNA into cells with no detectable toxicity. By tuning the nanoparticle formulation, enhanced detection can be achieved. This study is an important step towards rational design of materials to achieve specific interactions between biomolecules and synthetic nanoparticle surfaces.

Introduction

Materials that can selectively bind to biomolecules are crucial for biosensor development.[1-5] While the highest specificity is often achieved with biological receptors such as antibodies and aptamers,[6] developing synthetic nanoparticles for selective adsorption is also attractive. Such synthetic receptors provide higher stability at lower cost.[7] Indeed, many nanoparticle-based artificial enzymes (nanozymes),[7-12] inhibitors,[13,14] channels[15,16] and self-assembly systems[17] have already been demonstrated. However, selective binding of biopolymers using nanoparticles remains quite challenging. The main difficulty lies in the fact that most nanomaterials can only interact with biopolymers via relatively non-specific forces, leading to poor selectivity.[18-22] We reason that this problem might be overcome by introducing more specific intermolecular forces based on the properties of the target molecules. For this purpose, DNA is an ideal model target to obtain fundamental insights since arbitrary sequences and modifications are readily accessible through chemical DNA synthesis.

DNA is a negatively charged polymer with four types of nucleobases that can interact with materials via a number of intermolecular forces. Ideal receptors should have good sequence specificity, tunable adsorption strength and high biocompatibility. The previous works are summarized below based on different levels of specificity. First, cationic nanoparticles are an obvious choice for adsorbing negatively charged DNA. However, simple electrostatic interactions cannot easily distinguish between single-stranded (ss) and double-stranded (ds) DNA or between different DNA bases. In addition, cationic

particles are toxic to cells. Interestingly, many negatively charged materials adsorb DNA as well. For example, citrate-capped gold nanoparticles (AuNPs) strongly bind to DNA bases.[18-22] Negatively charged graphene oxide (GO) adsorbs DNA via hydrophobic interactions, hydrogen bonding and π-π stacking.[23-25] In both cases, ss-DNA adsorbs much faster than ds-DNA.[26,27] Certain base specificity can also be achieved (e.g. A and C bind to gold more strongly than T and G). The best sequence specificity is obtained with immobilized probe DNAs, where in principle only the complementary strands can be adsorbed.[28] However, the cost of such materials is very high. The question we aim to address herein is whether sequence specificity can be achieved without performing DNA grafting. To design such materials, an intuitive choice is to use nucleobases and their derivatives since they may form hydrogen bonding and base pairing interactions with target DNA. Another possibility is metal ion coordination, since DNA can bind to both soft and hard metals at different positions.[29-31] Therefore, to rationally design DNA receptors, nucleobase coordinated materials appear to be a good starting point (Figure 1B).

Mixing nucleobases and metal ions can induce polymerization to form nanoparticles (so called coordination polymers or CP). In general, CPs refer to hybrid materials formed by metal ion with bridging ligands.[32] High biocompatibility might be achieved by using amino acids and nucleotides to complex with non-toxic metal ions.[33] CPs have found many applications for gas adsorption, sensing, drug delivery and catalysis, but their DNA binding property has not been explored. Adenine and its derivatives are versatile building blocks,[34-36] where this base coordinates with many transition metal ions and forms crystalline or non-crystalline nanoparticles.[37-40] Recently, lanthanides and nucleotides

have been reported to form nanoparticles through both the bases and the phosphate.[41,42] In this paper, we investigate nucleotide containing CPs and demonstrate that sequence specificity and interaction strength can be tuned by rational design of their composition. The resulting materials are useful for developing biosensors for DNA detection.
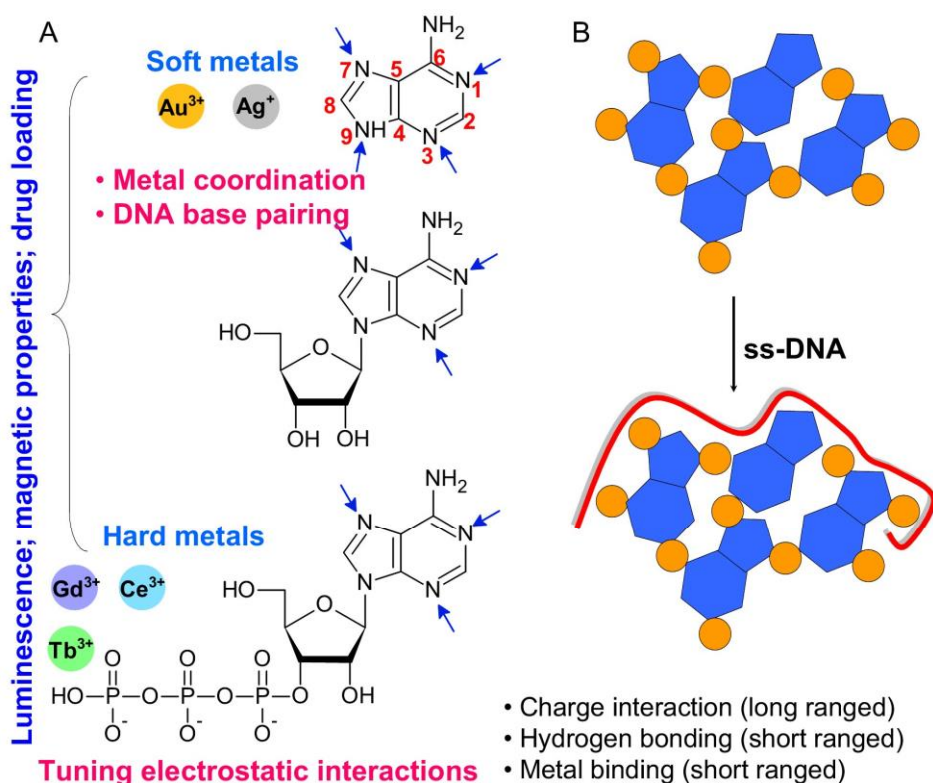
Figure 1. (A) Structures of adenine, adenosine and ATP and their interactions with metal ions through base coordination (blue arrows indicate possible metal binding sites) and through electrostatic interactions on the phosphate. The property of their complexes with metals can be further tuned by using different metal ions. (B) Schematics of the adenine/Au complex binding to ss-DNA, where the DNA can interact with both the base (blue polygons) and the metal ion (orange dots).

Materials and Methods

Chemicals. All of the DNA samples were purchased from Integrated DNA Technologies (IDT, Coralville, IA) and purified by standard desalting (see Table 1 for sequences). Chloroauric acid trihydrate was purchased from Fisher Scientific. Silver nitrate, terbium(III) chloride hexahydrate, cerium(III) chloride heptahydrate, gadolinium(III) chloride hydrate, adenine, adenosine 5′monophosphate (AMP) disodium salt, adenosine 5′-triphosphate (ATP) disodium salt hydrate, guanosine 5′-monophosphate (GMP) disodium salt hydrate, guanosine 5′-triphosphate (GTP) sodium salt hydrate, and 3-(4,5-

dimethylthiazol-2-yl)-2,5-diphenyltetrazolium bromide (MTT) were obtained from Sigma-Aldrich. Adenosine, 4-(2-hydroxyethyl)-1-piperazineethanesulfonic acid (HEPES) and NaCl were purchased from Mandel Scientific (Guelph, ON). 4',6-diamidino-2-phenylindole (DAPI) was from Life Technologies. Milli-Q water was used to prepare all the buffers and solution. All other reagents and solvents were of analytical grade and used as received.

Table 1. DNA samples used in this work.

DNA name	Sequences and modifications (from 5□ to 3□)
FAM-DNA1	FAM-ACGCATCTGTGAAGAGAACCTGGG
cDNA1	CCCAGGTTCTCTTCACAGATGCGT
Mismatch1	CCCAGGTTCTCTTCACACATGCGT
Mismatch2	CCCAGCTTCTCTTCACACATGCGT
FAM-A_{15}	FAM- AAAAAAAAAAAAAAA
FAM-T_{15}	FAM- TTTTTTTTTTTTTTT
FAM-C_{15}	FAM-CCCCCCCCCCCCCCC
FAM-G_{15}	FAM-GGGGGGGGGGGGGGG
A_{15}	AAAAAAAAAAAAAAA
T_{15}	TTTTTTTTTTTTTTT

Preparation of coordinated materials. The adenine/Au complexes were prepared by adding 100 μL adenine (50 mM) into 800 μL Milli-Q water. HAuCl$_4$ (100 μL, 50 mM) was then added to produce the 1:1 molar ratio complex. Precipitants were observed within several minutes. The samples with molar ratio of adenine-to-Au of 1:2, 1:3 and 1:4 were prepared in the similar method, where the concentration of adenine was fixed at 5 mM and HAuCl$_4$ was varied. Other nucleotide/metal complexes with 1:1 molar ratio of different nucleotide to Ag, Gd, Ce or Tb were also prepared using the same procedures. The

samples were centrifuged and washed with water to remove remaining chemicals. Freshly prepared samples were used for the experiments.

DNA adsorption. DNA adsorption kinetics was measured in buffer A (300 mM NaCl and 10 mM HEPES, pH 7.6) with FAM-DNA1 (20 nM) and adenine/Au complex (adenine=50 μM). The fluorescence intensity was monitored for 90 min using a fluorescence microplate reader by exciting at 485 nm (Infinite F200 Pro, Tecan). Control experiments were also performed with only 10 mM HEPES buffer without any NaCl. To study adsorption by adenosine/Au, a final of 20 nM FAM-T_{15} was added to 50 μM adenosine/Au complex in 0, 30, 100, and 300 mM NaCl. To test ss- versus ds-DNA, FAMDNA1 was fixed at 1 μM and an equal amount of its cDNA was mixed and then hybridized at 70 $^\circ$C to form ds-DNA. After that, the ds-DNA (20 nM) or FAM-DNA1 alone (20 nM) was mixed with adenine/Au (1:1) in buffer A.

DNA detection. For the sensitivity, the probe DNA (FAM-DNA1) was fixed at 1 μM and the different concentrations of the cDNA (2, 1, 0.5, 0.25, 0.1, 0.05 μM) were respectively mixed with FAM-labeled DNA and then hybridized at 70 $^\circ$C and formed ds-DNA. After the samples were cooled to room temperature, these samples (final concentration of DNA1=20 nM) were mixed with adenine/Au complex (50 μM) in buffer A. The fluorescence of these samples was monitored for 90 min using the microplate reader. To test different probe sequence, 10 μM FAM-A_{15} and T_{15} (or FAM-T_{15} and A_{15}) were hybridized to form ds-DNA. Then, these ss-DNA or ds-DNA (100 nM) were mixed with adenine/Au (50 μM) for 30 min in buffer (100 mM NaCl and 10 mM HEPES). The fluorescence emission spectra were recorded using a Varian Eclipse fluorometer with an excitation wavelength at 485 nm. Additional methods are in Supporting Information.
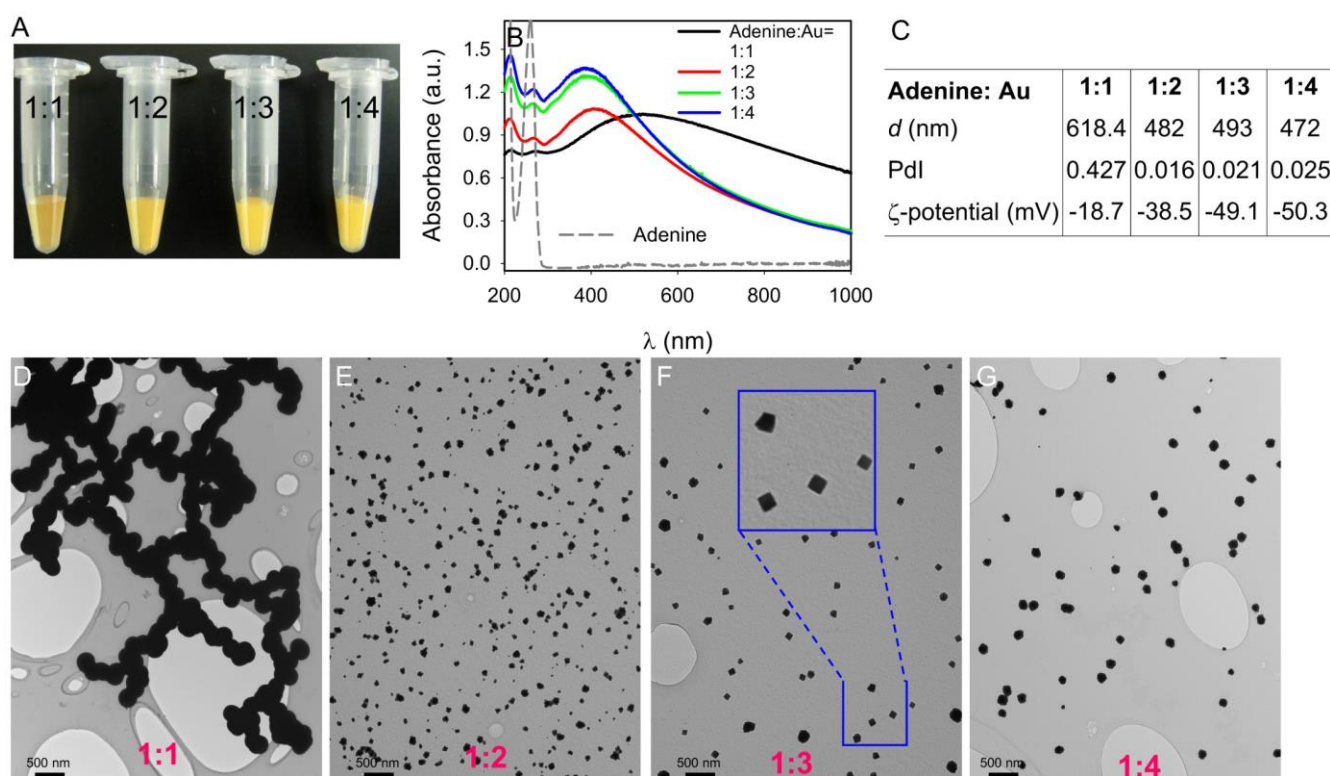
Results and Discussion

Adenine/Au complexes. There are many choices of both DNA bases and metal ions, where different combinations and even ratios might result in different DNA binding properties. Since adenine has been extensively used for metal coordination,[34-36] especially with gold,[37] we first tested this combination. Since each adenine has four metal binding sites (Figure 1A) and each gold ion can also bind several adenines, the ratio of these two was systematically varied. With the molar ratios of 1:2, 1:3, and 1:4 between adenine and $HAuCl_4$, yellow precipitants were observed in a few minutes for all the samples (Figure 2A), indicating the formation of CPs. The sample appeared to be slightly darker for the 1:1 ratio sample. The precipitants were washed in water and characterized by UV-vis spectroscopy (Figure 2B). With the 1:1 ratio, a broad absorption feature centered at ~500 nm is observed. For the other samples with more gold, the peak is shifted to 380 nm, suggesting two different coordination environments depending on the ratio. This absorption feature is attributed to the charge transfer between adenine and gold, while the original adenine absorption at 260 nm disappeared for all the samples (dashed line). The 380 nm peak is more intense with higher gold concentration, suggesting a more complete reaction. After centrifugation, we measured the supernatant absorption and determined the adenine:Au ratio is close to 1:1 in the CP for the 1:1 sample. On the other hand, the 1:3 and 1:4 ratios give a ratio of 2 adenine: 3 Au in the CP. This suggests that each adenine uses 3 sites to coordinate with Au and each Au binds to 2 adenines. All the four samples show a high background (e.g. the absorbance is >0.2 even at 1000 nm), indicating the presence of large particles that scatter light. Therefore, the samples were further analyzed using dynamic light scattering (DLS, Figure 2C). The hydrodynamic size of these particles is around 500 nm and decreases only slightly with increasing gold.

TEM micrographs of the dried samples show that at the 1:1 ratio, the particles are spherical (Figure 2D). At higher ratios, the morphology became irregular and it is interesting to note some nanocubes are form for the 1:3 sample (Figure 2F). This is again consistent with the UV-vis results of two different types of coordination structures. The DLS sizes are larger than the TEM measurements, suggesting aggregation

of the particles solution, which often dominates the light scattering signal. The particles remained stable after sonication or heating (Figure S1). ζ-potential measurement indicates that all the particles are negatively charged, and the absolute value of ζ-potential increases with increasing gold concentration (Figure 2C). With excess amount of gold, the particle surface is likely to be terminated with gold species. The increased negative charges suggest that these surface gold species are negatively charged, which is reasonable since these gold are likely to be extensively coordinated by Cl^- (e.g. the source of gold is $HAuCl_4$).

| Adenine: Au	1:1	1:2	1:3	1:4
d (nm)	618.4	482	493	472
PdI	0.427	0.016	0.021	0.025
ζ-potential (mV)	-18.7	-38.5	-49.1	-50.3

Figure 2. (A) Photographs of adenine coordinated Au complexes at different molar ratios of adenine:$HAuCl_4$. (B) UV-vis spectra of the adenine/Au complexes and free adenine. (C) DLS measurement of the hydrodynamic size and ζ-potential of the complexes. PDI means the polydispersity index. (D-G) TEM micrographs of the samples in (A). Scale bars = 500 nm. The blue boxed area in (F) shows a high magnification of this region.

DNA adsorption. To test these adenine/Au nanoparticles for DNA adsorption, a 6-carboxyfluorescein

(FAM)-labeled ss-DNA with a random sequence (FAM-DNA1, see Table 1 for sequence) was added and

its fluorescence intensity decreased gradually, regardless of the adenine/Au ratio (Figure S2, Supporting

Information). Fluorescence quenching is an indication of DNA adsorption as observed with

many other materials.[18,43,44] However, the final fluorescence did not drop to zero, suggesting either

incomplete adsorption or inefficient fluorescence quenching or both. To understand the quenching

mechanism, we measured fluorescence lifetime, which decreased from 4.2 ns for the free DNA to ~1.3

ns for the adsorbed DNA, suggesting dynamic quenching mechanism (Figure S3). This could be related

to the energy transfer from FAM to the adenine/Au complex, whose absorption spectrum overlaps with

the FAM emission at 520 nm. This is different from the quenching induced by graphene or AuNPs,

where it is generally accepted to be static quenching for adsorbed fluorophores.[18,43,44] To further confirm

adsorption, we measured fluorescence anisotropy of the free DNA (0.016) and after mixing with the

adenine/Au (0.152), which is also consistent with DNA binding to a large nanoparticle.

After demonstrating DNA adsorption with a random sequence, we next tested sequence

specificity. With the adenine/Au complexes, one might expect a more favorable interaction with a polyT

DNA if the Watson-Crick base pairing is still involved. Indeed, with 300 mM NaCl, FAM-T_{15} shows the

fastest fluorescence drop, suggesting that the A-T base pairing might still play a role even though the

adenines are complexed with gold (Figure 3A). Note that in a typical Watson-Crick A-T base pair, only

the exocyclic amine and the N1 nitrogen are used for base pairing. The exocyclic amine is typically not

responsible for metal coordination since its lone pair electron is delocalized into the purine ring.

Therefore, as long as a fraction of the surface adenines have free N1 sites, base pairing with thymine can

take place. The fluorescence of FAM-G_{15} only decreases slightly, which might be related to its tendency

to form quadruplex structures. It needs to be noted that poly-T DNA is usually a weak binder for most

materials (e.g with AuNPs or graphene oxide).[22] Therefore, it is quite remarkable to have a material that binds to poly-T DNA more favorably. To further understand the adsorption mechanism, the same experiment was repeated in the absence of salt (Figure 3B), where little adsorption was observed for all the sequences. This can be explained by the anionic nature of the adenine/Au complex and salt is required to overcome the long-ranged electrostatic repulsion. As long as the DNA could approach the complex surface, attractive forces such as hydrogen bonding and metal coordination might dominate the interaction. We further measured the adsorption of DNA by the adenosine/Au complex. The difference between adenosine and adenine is that the N9 nitrogen is occupied by the ribose for adenosine (Figure 1A), but their properties are quite different. For example, we recently reported that adenosine/Au complexes display interesting luminescence properties after UV light activation,[45] while adenine/Au is almost non-fluorescent. In addition, the adenosine/Au complex is non-charged, which suggests that the negative charge from the adenine/Au is related to the N9 nitrogen as well. In the adenosine/Au complex, very fast adsorption was observed and fluorescence was effectively quenched in a few minutes (Figure 3C). Adding salt actually decreased the amount of fluorescence quenching since adsorption is not limited by charge repulsion in this case. Other DNA sequences can also be quickly adsorbed by adenosine/Au, where poly-G DNA still displayed the slowest adsorption (Figure S4).
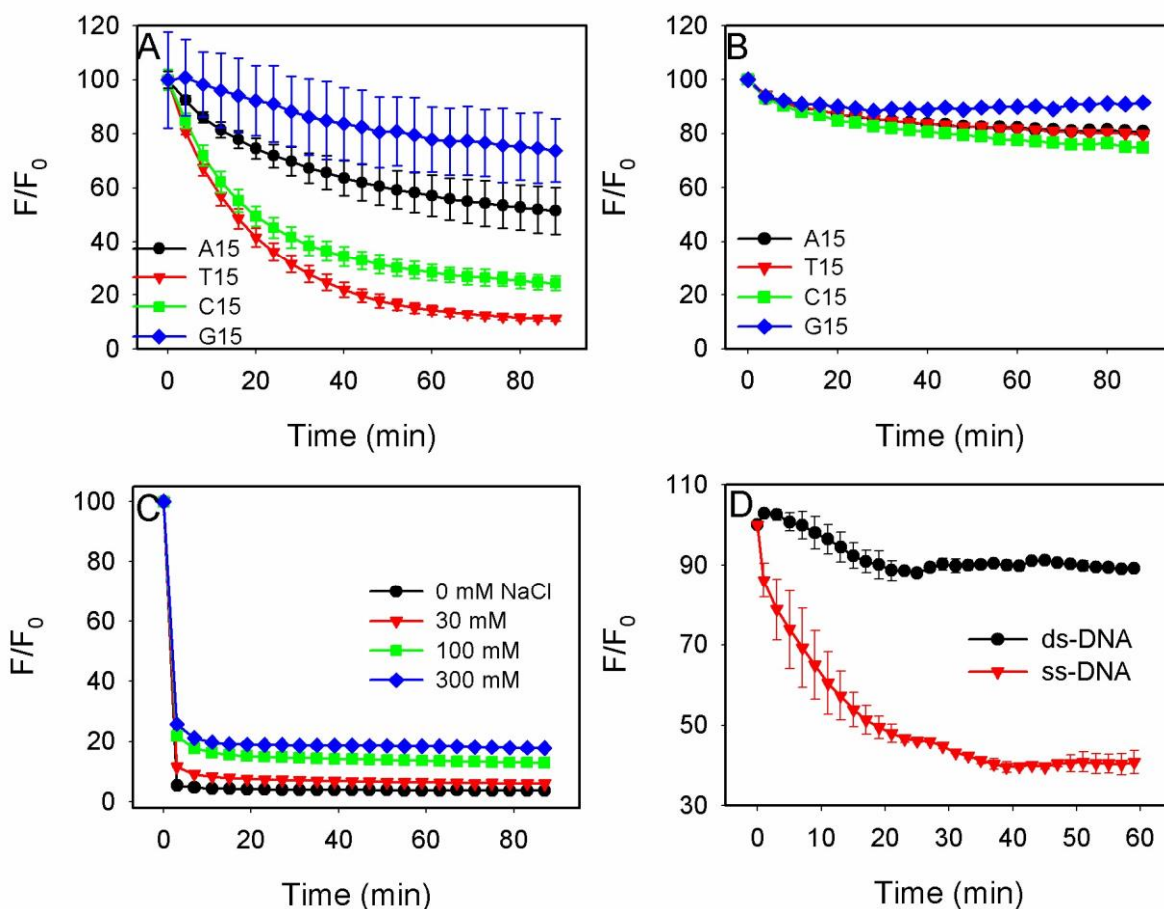
Figure 3. Adsorption of FAM-labeled A_{15}, T_{15}, C_{15} and G_{15} by the 1:1 adenine/Au complex in 300 mM NaCl (A) or without NaCl (B). Both samples contained 10 mM HEPES (pH 7.6) buffer. Adsorption is accompanied by fluorescence quenching. (C) Adsorption of FAM-T_{15} by adenosine/Au complex in different salt concentrations. (D) Adsorption of ss- and ds-DNA by the 1:1 adenine/Au complex.

The above experiments indicate that the adenine/Au complex might have certain sequence selectivity. In other words, the adenine base is partially responsible for DNA adsorption. These properties might allow the adenine/Au complex to distinguish between ss- and ds-DNA. To test this, we mixed a ds-DNA with the 1:1 adenine/Au complex (Figure 3D). The fluorescence of the ds-DNA does not decrease much even with 300 mM NaCl while strong quenching was observed for the ss-DNA.

Therefore, ss-DNA adsorbs much faster to the complex, confirming the base adsorption mechanism.

DNA binding to other nucleotide/metal complexes. While the fastest binding of poly-T DNA to the adenine/Au complex might suggest that the Watson-Crick base pairing remains effective even in the complex, more examples are needed to test generality. Towards this goal, we prepared a series of nucleobase and nucleotide coordinated complexes; their surface charge and particle sizes are listed in Table 2. Other than gold and silver, we failed to obtain adenine complexes with other transition metal ions. By using lanthanides and nucleotides, more complexes were formed. These materials can be classified based on their charge. For example, the adenine/Ag complex is positively charged and so are many of the AMP/lanthanide complexes, while AMP/Gd is almost charge neutral. Anionic complexes are formed when ATP or GTP were used to increase the number of negative charges. Therefore, by simply changing the composition of nucleotide and metal ions, we already have access to a broad range of surface chemistries. Many of the positively charged lanthanide complexes formed gel-like precipitant, which explains their very large particle size measured by DLS. The FAM-labeled DNA homo-polymers were used to study DNA adsorption.

Table 2. Complexes formed by mixing different metal ions and nucleobases/nucleotides and their size and surface charge.

Metal ion	Ag(I)	Gd(III)	Gd(III)	Gd(III)	Ce(III)	Ce(III)	Ce(III)	Tb(III)	Tb(III)
Nucleobase or nucleotide	Adenine	AMP	ATP	GMP	AMP	GMP	GTP	AMP	GTP
Size (nm)	68.4	2333	97	2836	4466	4925	456	4235	429
ζ-potential (mV)	24.1	-0.135	-5.01	4.3	5.91	9.37	-26.7	10.6	-24.6

As shown in Figure 4A, FAM-T_{15} quickly adsorbed to the negatively charged ATP/Gd complex, which is again consistent with the thymine/adenine interaction. The other three DNA molecules failed to bind. Compared to the adenine/Au complex, ATP/Gd has an even stronger preference for the poly-T DNA. This might be related to that DNA bases bind to Au more strongly than to Gd. In other words, DNA base pairing might be the main force for DNA adsorption by ATP/Gd. To test another type of nucleotide, we next studied GTP/Ce, which is also negatively charged (Figure 4B). In this case, the fastest adsorption was achieved with FAM-C_{15}, consistent with the guanine/cytosine interaction. FAMG$_{15}$ also showed moderate binding, while the other two DNA sequences failed to bind.

For positively charged or neutral complexes, however, DNA base pairing appears to play a less important role. For example, the cationic adenine/Ag complex showed similar adsorption for poly-A, T and C DNA, while its binding to G_{15} was the slowest (Figure 4C). The cationic GMP/Ce complex showed similar kinetics for all the sequences (Figure 4D). These experiments reveal an important design principle for such materials. To achieve sequence specificity, the material needs to be negatively charged to avoid non-specific electrostatic attraction. From the materials we have prepared so far, Watson-Crick base pairing has been obeyed as long as the material is negatively charged, suggesting that the surface nucleotides behave similarly to that in a DNA in terms of molecular recognition.
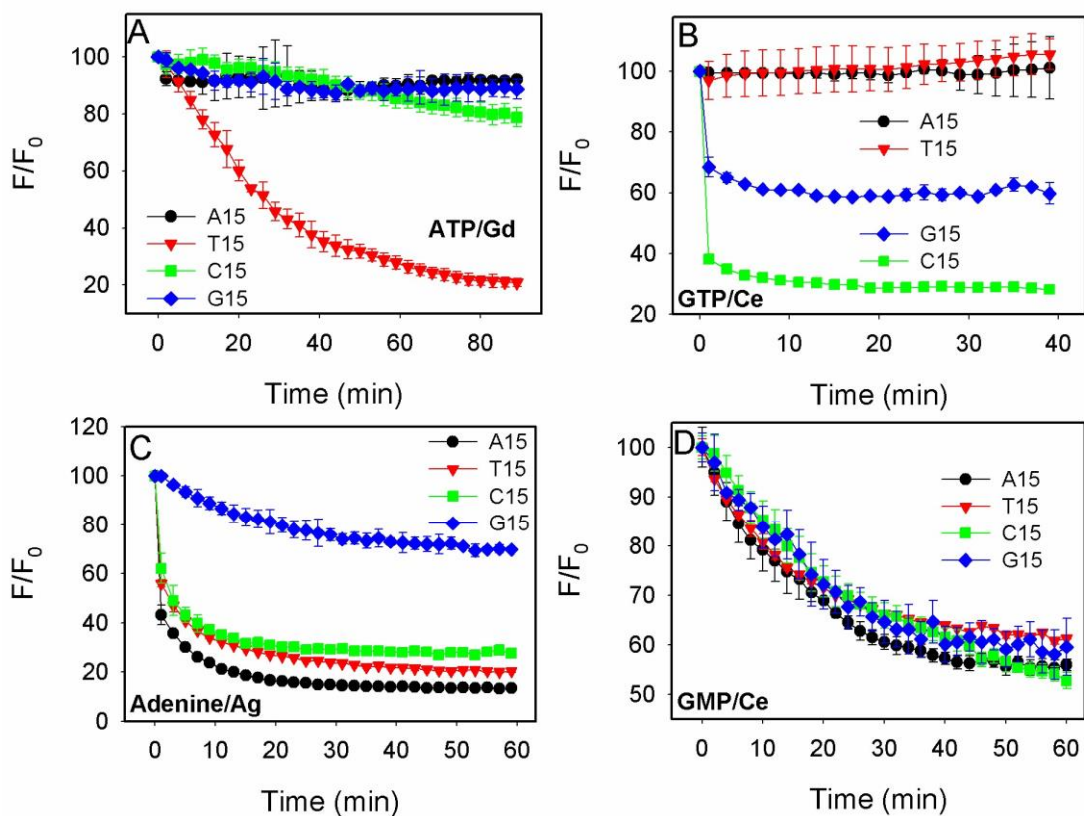
Figure 4. Adsorption of FAM-labeled A_{15}, T_{15}, C_{15} and G_{15} by (A) negatively charged ATP/Gd; (B) negatively charged GTP/Ce; (C) positively charged adenine/Ag and (D) positively charged GMP/Ce monitored by fluorescence quenching.

Metal ion directed binding affinity. Our above work has focused on the role of nucleotides for DNA adsorption. The other half of the material is metal ions that could also be important. For example, a simple switching from gold to silver has inverted the charge of the adenine complexes from negative to positive. At this moment, it is unclear whether metal ions are directly involved in DNA binding or not. If so, we reason that the binding strength between the nanoparticles and DNA can be further tuned by the choice of different metal ions. To quantitatively measure DNA adsorption affinity, we performed thermal desorption experiments by gradually heating the samples with pre-adsorbed FAM-labeled DNA and

monitoring fluorescence increase due to DNA desorption. Interestingly, the adenine/Au complex adsorbs DNA very tightly and DNA does not desorb even at 95 □C (Figure 5A). On the other hand, the lanthanide complexes showed desorption profiles similar to DNA melting curves, where desorption occurred over a broad temperature range spanning ~30 □C. A better analysis was made by plotting the first derivative of the curves (Figure 5B), where all the samples showed two melting transitions and subtle differences between different lanthanides were also observed. For example, the main transitions of the Gd and Ce complexes are at ~60 □C while the Tb complex has it main transition at ~50 □C. This subtle difference could be related to the affinity between the lanthanides and the adsorbed DNA. While we have not assigned the molecular origin of these transitions, it is quite certain that both metal ions and nucleotides are involved in DNA binding. The nucleotide interaction is more important for adsorption kinetics and base specificity, while metal binding is important for the adsorption affinity or thermodynamics. Au binds DNA with a much stronger affinity than lanthanides do.
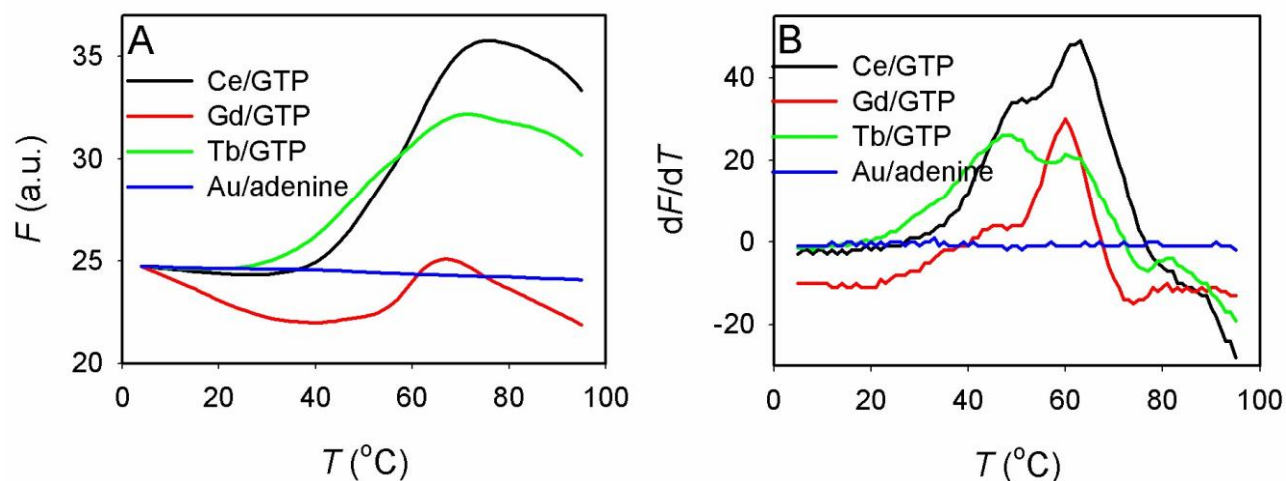

Figure 5. (A) Thermally induced DNA desorption. FAM-A$_{15}$ with Au/adenine and FAM-C$_{15}$ with the other three complexes. (B) The first derivatives of the melting curves in (A).

DNA sensing. After understanding the DNA recognition properties of the CPs, we next explored their analytical applications. The ability of the adenine/Au to distinguish between ss- and ds-DNA and its fluorescence quenching ability suggest its DNA sensing application. The sensing scheme is in Figure 6A. Using FAM-DNA1 as probe, we hybridized it with various concentrations of cDNA (Figure 6B). The decay of fluorescence was slower with increasing target DNA concentration. When the intensity at 30 min is plotted, a linear relationship is obtained until 20 nM target DNA is reached (Figure 6C). Further increase of the target DNA concentration did not bring much more change in the signal since the probe DNA was saturated. Based on the initial linear relationship, the detection limit was calculated to be 5 nM cDNA based on the signal greater than three times of the standard deviation of background. We further studied the adenine/Au complex for detecting mismatches (Figure 6D). The fluorescence changed very little with the perfect cDNA. With two base mismatches, there was a significant fluorescence decrease, and the one base mismatched DNA showed an intermediate response.

With the unique sequence specificity, we can demonstrate another level of control for DNA detection. For example, if we use FAM-A_{15} as the probe DNA to detect T_{15}, a very poor result is obtained (Figure 6E) since the signal in the presence or absence of the target DNA T_{15} is very similar. This is because the adsorption of FAM-A_{15} by the adenine/Au complex is unfavorable. On the other hand, if FAM-T_{15} is used as the probe DNA, A_{15} can significantly suppress fluorescence quenching (Figure 6F). This is because the adenine/Au complex adsorbs FAM-T_{15} and repels A_{15}. This experiment further confirms the specific DNA receptor function of the adenine/Au complex.
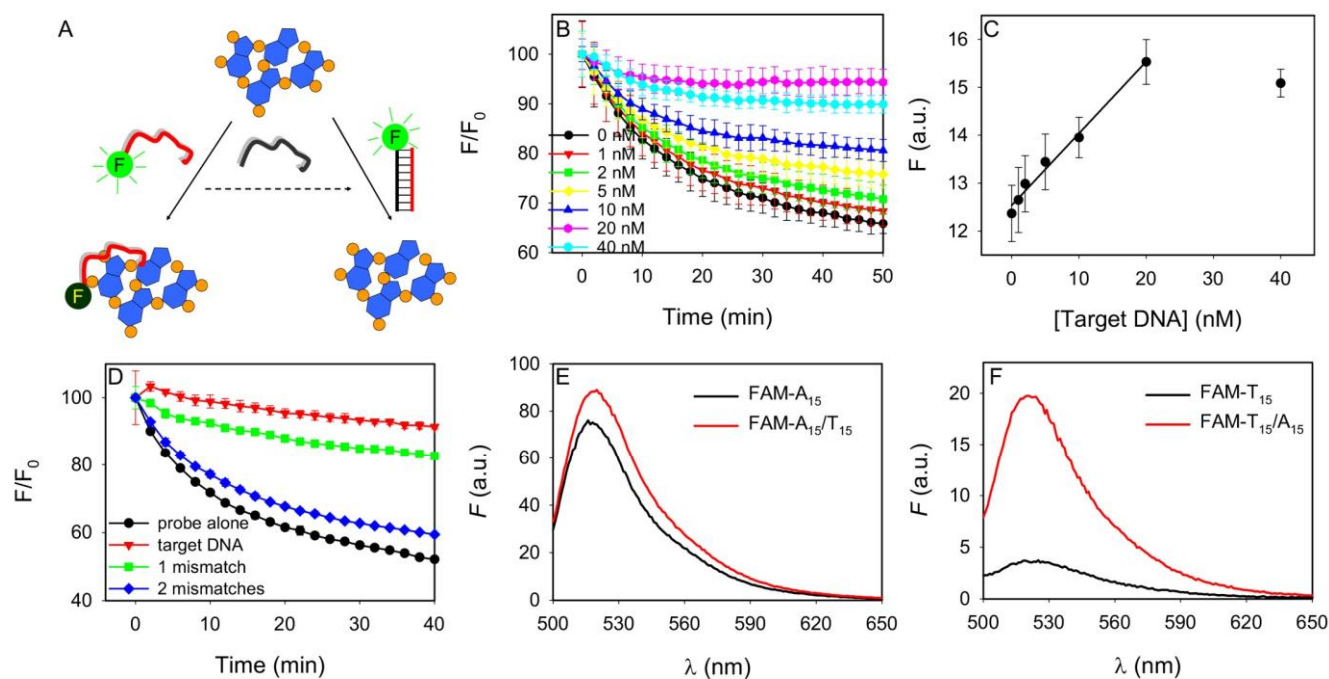
Figure 6. (A) Using adenine/Au complex for DNA detection. Adsorption of ss-DNA probe induces fluorescence quenching. While forming duplex DNA with the target can inhibit DNA adsorption. (B) Kinetics of fluorescence quenching with various concentrations of the target DNA in the presence of the 1:1 adenine/Au complex. (C) Sensitivity of the sensor measured at 30 min incubation time. (D) Sensor specificity test. Fluorescence spectra of the sensor response when FAM-A_{15} is used as a probe to detect T_{15} (E) or FAM-T_{15} is used as the probe to detect A_{15} (F). A larger difference in fluorescence intensity indicates a better sensor.

DNA release and delivery. Our above studies indicate that the adenine/Au complex can adsorb DNA strongly. Therefore, this complex might be useful for delivery of DNA into cells. Inside a cell, there are many thiolated compounds that might disrupt the complex. For example, when we mixed the complex with GSH, a high concentration tripeptide inside cells, fast increase of fluorescence indicating dissociation of the complex was observed (Figure 7A). But without GSH, the fluorescence remained low and stable. Figure 7C illustrates a relatively high intracellular accumulation of FAM-DNA1 and

adenine/Au complex and release of the FAM-DNA1 in HeLa cells. When incubated with FAM-DNA alone in the absence of the complex, no green fluorescence was observed in cells (Figure 7D), suggesting the complex delivered the DNA. It is also worthy of pointing out that adenine/Au or its DNA complex did not exhibit obvious cytotoxicity to HeLa cells after 72 h incubation (Figure 7B).
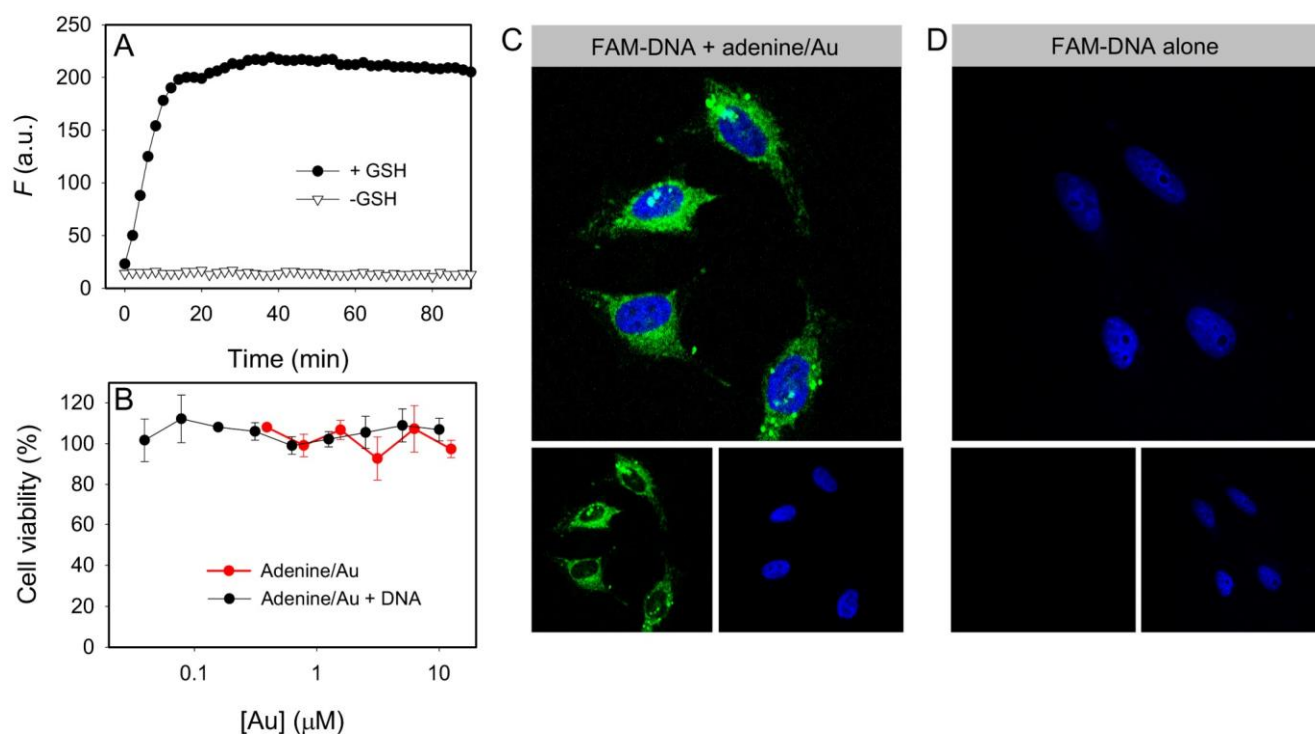
Figure 7. (A) In vitro release of FAM-DNA1 using 10 μM GSH from the adenine/Au complex at pH 7.4 (10 mM HEPES buffer). Without adding GSH, no DNA release is detected. (B) MTT assay of HeLa cells after treatment with adenine/Au complex or DNA/adenine/Au for 72 h. Confocal fluorescence micrographs of HeLa cells incubated with FAM-DNA/adenine/Au complex (C) or FAMDNA alone (D) for 4 h. The dose of FAM-DNA or its equivalent was ~28 nM in the cell culture. The cells were counterstained with DAPI (blue) for the cell nucleus. (C) and (D) each contains three panels. The bottom panels are the green and blue channels and the upper panel is the merged picture.

Conclusions. In summary, we have demonstrated a new concept of developing artificial DNA receptors. Such materials could be used for DNA detection. In the past few decades, many materials have been used for DNA adsorption. One of the main motivations is to develop gene delivery vehicles and other applications that include DNA purification and detection. Most materials reported so far have rather poor specificity for DNA sequences. In this work, we showed that advanced materials can be engineered to control surface charge and more detailed chemical interactions based on hydrogen bonding and metal coordination. We already demonstrated that adsorption kinetics can be controlled using the Watson-Crick base pairing principle and tuning surface charge, while the adsorption strength can be controlled by the choice of metal ions. While this work employs nucleotides and nucleobases, the same principle is also applicable to amino acids and lipids. It is unlikely that the ultimate specificity can rival that of complementary DNA recognition or antibody/antigen interaction. One direction to bring this research forward is through pattern recognition. For example, by using various combinations in an array format, it may be able to mimic the human nose to obtain much more complex function.[46-49] Compared to many other types of materials currently used for this purpose, the incorporation of rationally designed interactions can improve specificity.

Supporting Information available. Additional methods, DNA adsorption kinetics and fluorescence lifetime measurement. This material is available free of charge via the Internet at http://pubs.acs.org.

References:

(1)   Rosi, N. L.; Mirkin, C. A. *Chem. Rev.* **2005**, *105*, 1547-1562.

(2)   Katz, E.; Willner, I. *Angew. Chem., Int. Ed.* **2004**, *43*, 6042-6108.

(3)   Liu, J.; Cao, Z.; Lu, Y. *Chem. Rev.* **2009**, *109*, 1948–1998.

(4)   Fang, X. H.; Tan, W. H. *Acc. Chem. Res.* **2010**, *43*, 48-57.

(5)   Lubin, A. A.; Plaxco, K. W. *Acc. Chem. Res.* **2010**, *43*, 496-505.

(6)   Wilson, D. S.; Szostak, J. W. *Annu. Rev. Biochem.* **1999**, *68*, 611-647.

(7)   Kotov, N. A. *Science* **2010**, *330*, 188-189.

(8)   Manea, F.; Houillon, F. B.; Pasquato, L.; Scrimin, P. *Angew. Chem., Int. Ed.* **2004**, *43*, 6165-6169.

(9)   Luo, W.; Zhu, C.; Su, S.; Li, D.; He, Y.; Huang, Q.; Fan, C. *ACS Nano* **2010**, *4*, 7451-7458.

(10)   Asati, A.; Santra, S.; Kaittanis, C.; Nath, S.; Perez, J. M. *Angew. Chem., Int. Ed.* **2009**, *48*, 2308-2312.

(11)   Gao, L.; Zhuang, J.; Nie, L.; Zhang, J.; Zhang, Y.; Gu, N.; Wang, T.; Feng, J.; Yang, D.; Perrett, S.; Yan, X. *Nat Nano* **2007**, *2*, 577-583.

(12)   Pautler, R.; Kelly, E. Y.; Huang, P.-J. J.; Cao, J.; Liu, B.; Liu, J. *ACS Appl. Mater. Inter.* **2013**, *5*, 6820–6825.

(13)   De, M.; Chou, S. S.; Dravid, V. P. *J. Am. Chem. Soc.* **2011**, *133*, 17524-17527.

(14)   Jin, L.; Yang, K.; Yao, K.; Zhang, S.; Tao, H.; Lee, S.-T.; Liu, Z.; Peng, R. *ACS Nano* **2012**, *6*, 4864-4875.

(15)   Chen, Z.; Jiang, Y. B.; Dunphy, D. R.; Adams, D. P.; Hodges, C.; Liu, N. G.; Zhang, N.; Xomeritakis, G.; Jin, X. Z.; Aluru, N. R.; Gaik, S. J.; Hillhouse, H. W.; Brinker, C. J. *Nat. Mater.* **2010**, *9*, 667-675.

(16)   Venkatesan, B. M.; Bashir, R. *Nat. Nanotechnol.* **2011**, *6*, 615-624.

(17)   Gao, Y.; Tang, Z. *Small* **2011**, *7*, 2133-2146.

(18)   Lu, C. H.; Yang, H. H.; Zhu, C. L.; Chen, X.; Chen, G. N. *Angew. Chem. Int. Ed.* **2009**, *48*, 4785-4787.

(19)   Herne, T. M.; Tarlov, M. J. *J. Am. Chem. Soc.* **1997**, *119*, 8916-8920.

(20)   Zhang, X.; Servos, M. R.; Liu, J. *Langmuir* **2012**, *28*, 3896-3902.

(21)   Wu, M.; Kempaiah, R.; Huang, P.-J. J.; Maheshwari, V.; Liu, J. *Langmuir* **2011**, *27*, 2731–2738.

(22)   Liu, J. *Phys. Chem. Chem. Phys.* **2012**, *14*, 10485-10496.

(23)   Varghese, N.; Mogera, U.; Govindaraj, A.; Das, A.; Maiti, P. K.; Sood, A. K.; Rao, C. N. R. *ChemPhysChem* **2009**, *10*, 206-210.

(24)   Tang, Z. W.; Wu, H.; Cort, J. R.; Buchko, G. W.; Zhang, Y. Y.; Shao, Y. Y.; Aksay, I. A.; Liu, J.; Lin, Y. H. *Small* **2010**, *6*, 1205-1209.

(25)   Park, J. S.; Na, H.-K.; Min, D.-H.; Kim, D.-E. *Analyst* **2013**, *138*, 1745-1749.

(26)   Li, H.; Rothberg, L. J. *J. Am. Chem. Soc.* **2004**, *126*, 10958-10961.

(27)   He, S. J.; Song, B.; Li, D.; Zhu, C. F.; Qi, W. P.; Wen, Y. Q.; Wang, L. H.; Song, S. P.; Fang, H. P.; Fan, C. H. *Adv. Funct. Mater.* **2010**, *20*, 453-459.

(28)   Elghanian, R.; Storhoff, J. J.; Mucic, R. C.; Letsinger, R. L.; Mirkin, C. A. *Science* **1997**, *277*, 1078-1080.

(29)   Barton, J. K.; Lippard, S. J. *Metal Ions in Biology* **1980**, *1*, 31.

(30)   Sigel, R. K. O.; Sigel, H. *Acc. Chem. Res.* **2010**, *43*, 974-984.

(31)   Zhang, X.-B.; Kong, R.-M.; Lu, Y. *Annu. Rev. Anal. Chem.* **2011**, *4*, 105-128.

(32)   Whittell, G. R.; Hager, M. D.; Schubert, U. S.; Manners, I. *Nat. Mater.* **2011**, *10*, 176-188.

(33)   Liu, Y.; Tang, Z. *Chem. Eur. J* **2012**, *18*, 1030-1037.

(34)   Verma, S.; Mishra, A. K.; Kumar, J. *Acc. Chem. Res.* **2009**, *43*, 79-91.

(35)   Prizant, L.; Olivier, M. J.; Rivest, R.; Beauchamp, A. L. *J. Am. Chem. Soc.* **1979**, *101*, 2765-

2767.

(36)   Gillen, K.; Jensen, R.; Davidson, N. *J. Am. Chem. Soc.* **1964**, *86*, 2792-2796.

(37)   Wei, H.; Li, B.; Du, Y.; Dong, S.; Wang, E. *Chem. Mater.* **2007**, *19*, 2987-2993.

(38)   Purohit, C. S.; Verma, S. *J. Am. Chem. Soc.* **2005**, *128*, 400-401.

(39)   Garcia-Teran, J. P.; Castillo, O.; Luque, A.; Garcia-Couceiro, U.; Roman, P.; Lezama, L. *Inorg. Chem.* **2004**, *43*, 4549-4551.

(40)   An, J.; Geib, S. J.; Rosi, N. L. *J. Am. Chem. Soc.* **2009**, *131*, 8376-8377.

(41)   Nishiyabu, R.; Hashimoto, N.; Cho, T.; Watanabe, K.; Yasunaga, T.; Endo, A.; Kaneko, K.; Niidome, T.; Murata, M.; Adachi, C.; Katayama, Y.; Hashizume, M.; Kimizuka, N. *J. Am. Chem. Soc.* **2009**, *131*, 2151-2158.

(42)   Tan, H.; Chen, Y. *Chem. Comm.* **2011**, *47*, 12373-12375.

(43)   Yang, R. H.; Jin, J. Y.; Chen, Y.; Shao, N.; Kang, H. Z.; Xiao, Z.; Tang, Z. W.; Wu, Y. R.; Zhu, Z.; Tan, W. H. *J. Am. Chem. Soc.* **2008**, *130*, 8351-8358.

(44)   Dubertret, B.; Calame, M.; Libchaber, A. J. *Nat. Biotechnol.* **2001**, *19*, 365-370.

(45)   Lopez, A.; Liu, J. *J. Phys. Chem. C* **2013**, *117*, 3653-3661.

(46)   Wright, A. T.; Anslyn, E. V. *Chem. Soc. Rev.* **2006**, *35*, 14-28.

(47)   Rakow, N. A.; Suslick, K. S. *Nature* **2000**, *406*, 710-713.

(48)   You, C.-C.; Miranda, O. R.; Gider, B.; Ghosh, P. S.; Kim, I.-B.; Erdogan, B.; Krovi, S. A.; Bunz, U. H. F.; Rotello, V. M. *Nat Nano* **2007**, *2*, 318-323.

(49)   Pei, H.; Li, J.; Lv, M.; Wang, J.; Gao, J.; Lu, J.; Li, Y.; Huang, Q.; Hu, J.; Fan, C. *J. Am. Chem. Soc.* **2012**, *134*, 13843-13849.